

PDF hosted at the Radboud Repository of the Radboud University Nijmegen

The following full text is a publisher's version.

For additional information about this publication click this link.

<http://hdl.handle.net/2066/29201>

Please be advised that this information was generated on 2019-11-22 and may be subject to change.

Magnetization of Mesoscopic Superconducting Disks

P. Singha Deo,* V. A. Schweigert,[†] and F. M. Peeters[‡]

Department of Physics, University of Antwerp (UIA), B-2610 Antwerpen, Belgium

A. K. Geim

High Field Magnet Laboratory, University of Nijmegen, 6525 ED Nijmegen, The Netherlands

(Received 25 April 1997)

Solutions of Ginzburg-Landau equations coupled with three-dimensional Maxwell equations reveal an intriguing magnetic response of small superconducting particles, qualitatively different from the two-dimensional approximation but in agreement with recent experiments. Depending on the radius and thickness, first or second order transitions are found for the normal to superconducting state. For a sufficiently large radius of the disk, several transitions in the superconducting phase are obtained which correspond to different angular momentum giant vortex states. The incorporation of the finite thickness in the calculation is crucial in order to obtain agreement with the position and the size of these jumps, and the line shape and magnitude of the magnetization curves. [S0031-9007(97)04781-9]

PACS numbers: 74.25.Ha, 74.60.Ec, 74.80.-g

Recent advances in microfabrication technology and measurement techniques have allowed the first studies of thermodynamic properties of well controlled mesoscopic superconducting particles [1–3]. The samples are mesoscopic in the sense that their size is comparable to the Ginzburg-Landau (GL) coherence length. Buisson *et al.* [1] performed magnetization measurements on an ensemble of disks with large separation between them in order to make the dipolar interaction between the disks negligible. They found oscillatory behavior in the magnetization near the superconducting transition temperature and showed that the linearized Ginzburg-Landau (LGL) equations are able to explain qualitatively part of their experiments but there are some major discrepancies in size and position of the jumps in the magnetization. Recently Geim *et al.* [3] used submicron Hall probes to detect the magnetization of *single* superconducting disks with size down to $0.1 \mu\text{m}$. At different applied fields the disks show various kinds of phase transitions within the superconducting state and between the superconducting and normal state which can be first or second order depending on the sample dimensions and temperature. The aim of this Letter is to explain this intriguing behavior and to give a quantitative analysis of these magnetization experiments.

A number of earlier works studied (1) disk geometries in the framework of the LGL equation where a uniform magnetic field is assumed [1,2,4] in the disks, or (2) cylindrical geometries in the framework of the non-linear GL equations [5]. The first type of approximation is reasonable if one is interested in the superconducting-normal state boundary where the order parameter is very small and the magnetic field equals the external one. The second type of approach is also valid away from this boundary but does not work for disks of finite thickness. Here we are interested to explain the full magnetization curve as a function of the external magnetic field for mesoscopic disks with finite thickness. Magnetization

is the ideal tool to understand the superconducting state deep inside the phase boundary.

It is known that a type-II superconducting cylinder in a magnetic field parallel to its axis can exist in three phases of superconductivity. Below H_{c1} we have a pure superconducting state, between H_{c1} and H_{c2} there is the mixed state, and between H_{c2} and H_{c3} we have surface superconductivity or the giant vortex state [6]. As the height of the cylinder is reduced, so that it becomes a disk, the magnetic field penetration into the sample is determined by the penetration length λ as well as the disk thickness, due to geometrical form factors. This makes the above simple divisions no longer applicable. Our problem requires a 3D solution, instead of their 2D version which turns out to be essential in order to understand the experiments of Refs. [1,3].

We consider superconducting *Al* disks ($\kappa = 0.28$) with radius R and thickness d immersed in an insulating medium. Thin film disks are known to behave as type-II samples [7] and can be described by the GL theory [1]. For mesoscopic *Al* samples (squares and thin wires), the GL theory has been successfully employed to explain the phase boundary [2]. Hence as a first approximation, neglecting the nonlocal effects, we solve the system of two coupled GL equations.

$$\frac{1}{2m} \left(-i\hbar\vec{\nabla} - \frac{2e\vec{A}}{c} \right)^2 \Psi = -\alpha\Psi - \beta\Psi|\Psi|^2, \quad (1)$$

$$\vec{\nabla} \times \vec{\nabla} \times \vec{A} = \frac{4\pi}{c} \vec{j}, \quad (2)$$

where the density of superconducting current \vec{j} is given by

$$\vec{j} = \frac{e\hbar}{im} (\Psi^* \vec{\nabla} \Psi - \Psi \vec{\nabla} \Psi^*) - \frac{4e^2}{mc} |\Psi|^2 \vec{A}. \quad (3)$$

The boundary conditions on the disk corresponding to zero current density in the insulator medium is

$$\left(-i\hbar\vec{\nabla} - \frac{2e\vec{A}}{c} \right) \Psi|_n = 0, \quad (4)$$

where the subscript n denotes the component normal to the disk surface. The boundary condition for the vector potential is such that far away from the superconducting disk the field equals the applied field $\vec{H} = (0, 0, H_0)$, i.e., $\vec{A}|_{\vec{\rho} \rightarrow \infty} = \vec{e}_\phi H_0 \rho / 2$. Here \vec{e}_ϕ denotes the azimuthal direction and ρ is the radial distance from the disk center.

Using dimensionless variables and the London gauge $\text{div} \vec{A} = 0$, we rewrite the system of Eqs. (1)–(4) into the following form:

$$(-i\vec{\nabla} - \vec{A})^2 \Psi = \Psi(1 - |\Psi|^2), \quad (5)$$

$$-\kappa^2 \Delta \vec{A} = \frac{1}{2i} (\Psi^* \vec{\nabla} \Psi - \Psi \vec{\nabla} \Psi^*) - |\Psi|^2 \vec{A}. \quad (6)$$

Here the distance is measured in units of the coherence length $\xi = \hbar / \sqrt{-2m\alpha}$, the order parameter in $\psi_0 = \sqrt{-\alpha/\beta}$, the vector potential in $c\hbar/2e\xi$, $\kappa = \lambda/\xi$ is the GL parameter, and $\lambda = c\sqrt{m/\pi}/4e\psi_0$ is the penetration length. We measure the magnetic field in $H_{c2} = c\hbar/2e\xi^2 = \kappa\sqrt{2}H_c$, where $H_c = \sqrt{-4\pi\alpha/\beta}$ is the critical field. The difference of the Gibbs free energy G between the superconducting and the normal states measured in $H_c^2 V / 8\pi$ can be expressed through the integral

$$G = \int [2(\vec{A} - \vec{A}_0) \cdot \vec{j} - |\Psi|^4] d\vec{r} / V, \quad (7)$$

over the disk volume $V = \pi R^2 d$, where $\vec{A}_0 = \vec{e}_\phi H_0 \rho / 2$ is the external vector potential, and $\vec{j} = (\Psi^* \vec{\nabla} \Psi - \Psi \vec{\nabla} \Psi^*) / 2i - |\Psi|^2 \vec{A}$ is the dimensionless superconducting current.

For thin disks, the magnetic field is uniformly distributed along the z direction. When the disk thickness becomes comparable to the penetration length, the magnetic field is expelled from the disk due to the Meissner effect. The field penetrates only a depth λ inside the disk. Therefore, the variation of the vector potential in the direction parallel to the applied field becomes rather strong for $d > \lambda$. Nevertheless, this does not lead to essential variations of the order parameter in this direction, in disks thinner than the coherence length. Representing the order parameter as a series $\Psi(z, \vec{\rho}) = \sum_k \cos(k\pi z/d) \Psi_k(\vec{\rho})$, which obeys the boundary condition (4) at the disk sides $z = \pm d/2$ and using the first GL Eq. (1), one can verify that the part of the order parameter which is uniform in the z direction, i.e., Ψ_0 gives the main contribution to the expansion for $(\pi\xi/d)^2 \gg 1$. Therefore, we may assume a uniform order parameter along the z direction and average the first GL equation over the disk thickness. Since the order parameter does not change in the z direction, both the superconducting current and the vector potential have no z component. Then the boundary condition (4) is automatically fulfilled on the upper and lower disk sides.

Our 3D calculations show that the disks studied experimentally in Ref. [1] exist in a regime of surface superconductivity, or the giant vortex state. If the thickness of the disks is further reduced then the giant vortex breaks up into many vortices if the radius of the disk is sufficiently large, even for a type-I sample.

Therefore, we consider the situation with a fixed value of the angular momentum L for the order parameter $\Psi(\vec{\rho}) = F(r) \exp(iL\phi)$, when both the vector potential and the superconducting current are directed along \vec{e}_ϕ . Then Eqs. (5) and (6) are reduced to the following form:

$$-\frac{1}{\rho} \frac{\partial}{\partial \rho} \rho \frac{\partial F}{\partial \rho} + \left(\frac{L^2}{\rho^2} - 2 \frac{L}{\rho} \langle A \rangle + \langle A^2 \rangle \right) F = F(1 - F^2), \quad (8)$$

$$-\kappa^2 \left(\frac{\partial}{\partial \rho} \frac{1}{\rho} \frac{\partial \rho A}{\partial \rho} + \frac{\partial^2 A}{\partial z^2} \right) = \left[\left(\frac{L}{\rho} - A \right) F^2 \right] \theta(r/R) \theta(2|z|/d), \quad (9)$$

where $\theta(x < 1) = 1$, $\theta(x > 1) = 0$; $\vec{A} = \vec{e}_\phi A$; R , d are the dimensionless disk radius and thickness, respectively; the brackets $\langle \rangle$ mean averaging over the disk thickness $\langle f(\rho) \rangle = \int_{-d/2}^{d/2} f(z, \rho) dz / d$.

The magnetic field created by the superconducting current in the disk decreases in strength away from the disk as a magnetic dipole field: $H \sim 1/r^3$. Because of this, in our numerical calculations the condition for the vector potential is transferred from infinity to the boundaries of the simulation region as follows: $A(z, r = R_s) = \frac{1}{2} H_0 R_s$, $A(|z| = d_s, \rho) = \frac{1}{2} H_0 \rho$, where $R_s, d_s \gg R, d$ are the sizes of the simulation region in the radial and z directions, respectively. The boundary conditions for the order parameter

$$\frac{\partial F}{\partial \rho} \Big|_{\rho=R} = 0, \quad \rho \frac{\partial F}{\partial \rho} \Big|_{r=0} = 0, \quad (10)$$

correspond to zero current density at the disk surface and a finite value of the first derivative of F at the disk center. To solve numerically the system of Eqs. (8) and (9) we apply a finite-difference representation of the GL and 3D Maxwell equations on the space grid ρ_i, z_j .

Disks in three different regimes will be considered: (1) type-II, (2) type-I, and (3) multiple type-I behavior. When we compare the theoretical results with the experimental data we have to keep in mind that experimentally the magnetization will depend on the filling fraction of the Hall bars used as detectors which is not exactly known. Also because of the square geometry of the Hall detector whose sides are of the same size as the diameter of the largest disk it will underestimate the magnetization (the flux expelled) of the smaller disks. These effects will result in an unknown scale factor for the magnetization of order 1. In order to have a comparison of relative magnitudes such as the size of the jumps in magnetization, we scale the theoretical results such that they have the same maximum magnetization as observed experimentally. When determining the magnetization from the LGL equation, the same method as in Ref. [1] was used; we have assumed the Abrikosov parameter β to be 1.0 as done in Ref. [1]. We compare our theoretical results with the experimental results on Al disks at 0.4 K of Geim *et al.* [3] and took for the

zero temperature coherence length $\xi(0) = 250$ nm and the penetration length $\lambda(0) = 70$ nm as estimated in Ref. [3]. The disk thickness and radius are also given in Ref. [3] and therefore our theory does not contain any fitting parameters.

Figure 1 shows the magnetization curves for an Al disk of thickness $d = 0.15$ μm and radius $R = 0.315$ μm . Large solid dots are the experimental data and exhibit a continuous superconducting-normal transition; the dotted curve is the solution from the LGL equation, whereas the thin solid curve is the numerical solution of the nonlinear GL equations coupled to the three-dimensional Maxwell equation. The dotted curve is scaled by 0.158 and the solid curve by 0.537. Surprisingly the dotted curve gives a line shape in closer agreement with the experiment but its magnitude is clearly too large. There is some improvement in the line shape (dashed curve) if we reduce the disk thickness to 0.07 μm in which case the radius of the disk was changed to 0.31 μm in order to keep the critical field the same (the magnetization was scaled by 1). Therefore, we suspect that the effective thickness of the disk which is still superconducting is much smaller than the actual thickness.

Figure 2 shows the magnetization curves for a larger disk of thickness 0.15 μm and radius 0.473 μm at 0.4 K. The same symbol and curve conventions are used as in the previous figure. The dotted curve is scaled by 0.124 and the thin solid curve by 0.581. It is obvious that the dotted curve is very different in shape and magnitude and shows a jump in magnetization at a very different value compared to the experimental curve. This clearly demonstrates that a LGL equation with a homogeneous magnetic field distribution over the disk is not appropriate in this case. The finite thickness of the disk results in very important geometrical corrections to the field profile which

influences the superconducting state appreciably. Note that the magnetic field dependence of the experimental curve is well described by the thin solid curve: (1) The slope of the magnetization curve, (2) the nonlinear behavior near the step in the magnetization, and (3) also the magnetic field at which the step in the magnetization takes place is correctly predicted. The experiment shows a first order transition from the superconducting to normal state at a magnetic field of 70.86 G while our calculations still predict a transition to the $L = 1$ superconducting state which becomes normal at 81.5 G. The origin of this small discrepancy is still not clear to us but may be due to effects of disorder [8].

The magnetization curves for a disk of thickness 0.15 μm and radius 1.2 μm is shown in Fig. 3. The symbol and the curve conventions are again the same as before. The dotted curve is scaled by 0.062 and the thin solid curve by 0.775 . Note that the LGL equation in this case gives the same type of discrepancies as found in the experiment of Buisson *et al.* [1]. First, they found that the magnitude of the jumps in the magnetization as obtained from a solution of the LGL equation is too large compared to the experimental results. Buisson *et al.* argued that this was due to an ensemble averaging in their experiment. The single disk experiment of Geim *et al.* rules out this possibility. It is true that the magnitude of the jumps in the single disk experiment is much larger than in the many disk experiment, but still, for the single disk, the jumps are much smaller than those obtained from a solution of the LGL equation (compare the dotted curve with the experimental data in Fig. 3). Our thin solid curve gives precisely the same magnitude for the jumps in the magnetization as in the experiment and also the correct magnitude of magnetization and magnetic field for most of the transitions. Second, they found that the position of the first jump in the magnetization obtained from the LGL equation is much below that of the experimental curve. No proper explanation could be given for this. Our dotted curve gives similar discrepancy of approximately the same

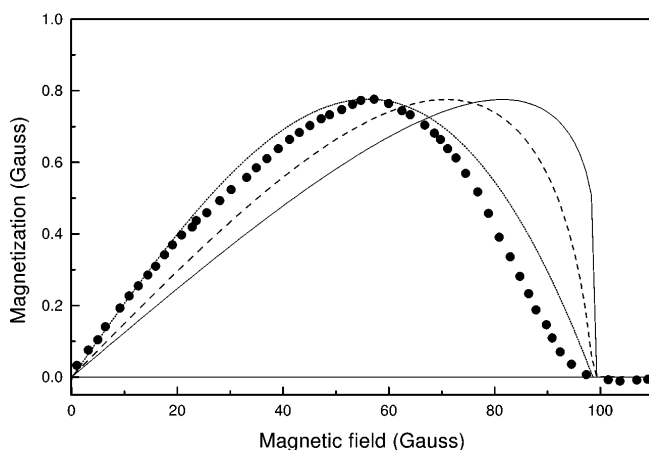


FIG. 1. Magnetization versus the external magnetic field for a superconducting disk of radius $R = 0.315$ μm and thickness $d = 0.15$ μm at $T = 0.4$ K. Solid dots are the experimental data from Ref. [3]. We show the results of the GL theory including the 3D Maxwell equation (solid curve, and dashed curve for $R = 0.31$ μm and $d = 0.07$ μm , respectively), and the result for the LGL theory (dotted curve).

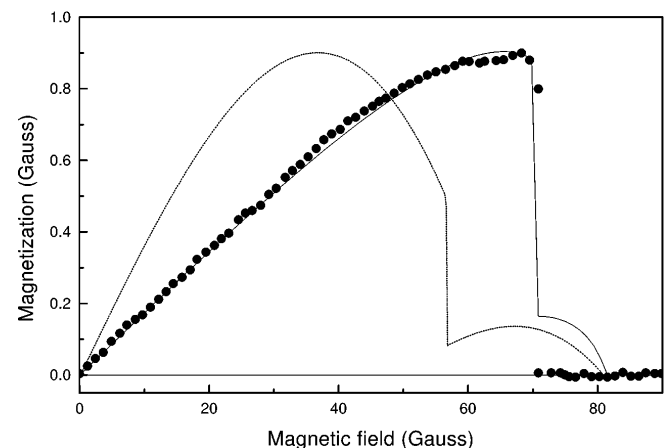


FIG. 2. The same as Fig. 1 but now for a disk with radius $R = 0.473$ μm and thickness $d = 0.15$ μm .

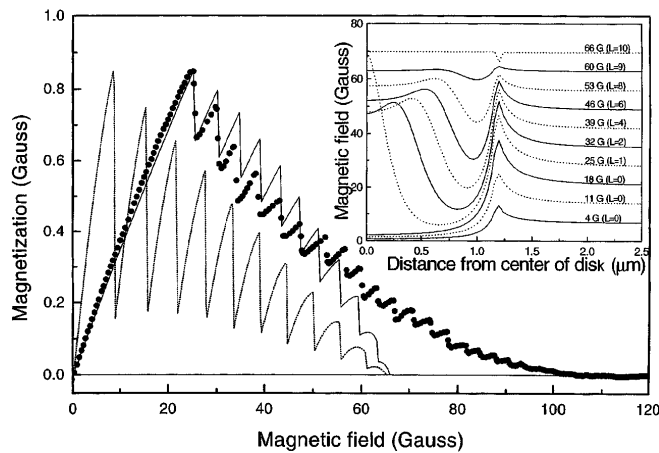


FIG. 3. The same as Fig. 1 for a disk of radius $R = 1.2 \mu\text{m}$ and thickness $d = 0.15 \mu\text{m}$. In the inset we show the field distribution in the plane through the center of the disk for different values of the external magnetic field. Far away from the center of the disk the magnetic field equals the external magnetic field.

magnitude and the thin solid curve settles this dispute. The first jump coincides with that of the experimental curve. We find that if we keep the radius unchanged and decrease the disk thickness then the upper critical field and the number of jumps in the magnetization curve remain unchanged. Only the position of the first peak shifts towards lower magnetic field which will of course also lead to an increase in the magnetic field spacing at which the jumps in magnetization occurs. This obviously is due to the fact that as the disk thickness is reduced the magnetic field inside the disk increases at a faster rate and so the transition to the first fluxoid state occurs at lower applied fields. Near the critical field of course the field inside does not depend on the thickness and is the same as the external field. This once again shows that the demagnetization factor is crucial for these disks and they determine largely the shape of the magnetization curves. Another interesting point to be noted is that the experimental curve shows a gradually decreasing interval of magnetic field at which the jumps occur. It was shown in Ref. [4] that within the LGL theory the flux quantization condition does not imply that the jumps in the magnetization will occur at regular intervals. As long as the order parameter at the central region of the disk is not negligible, the interval will decrease slowly and hence only for large values of L the interval will be the same as that given by the flux quantization condition. But our 3D solution shows a more drastic decrease in the interval. The reason is that at smaller fields the field inside the disk changes very slowly. In fact there is even a small regime where the field at the center of the disk can decrease with increasing applied field (see curves for $L = 1$ and $L = 2$ in the inset of Fig. 3). In the inset of Fig. 3 we have plotted the magnetic field distribution $H(\rho, z = 0, \theta = 0)$ of the system considered in Fig. 3 for ten values of the applied field. The corresponding value of the angular momentum

of the equilibrium superconducting state and the magnetic field is also indicated. For $L \neq 0$ there is substantial penetration of the magnetic field in the center of the disk while a ringlike region near the edge of the disk remains superconducting.

All along we have assumed that the system evolves along the free energy minimum and obtained quantitative agreement for the position, magnitude, and periodicity of the jumps in the magnetization as well as the absolute value of the magnitude of magnetization. But there is one discrepancy. Note that the theoretical curves in Fig. 3 show a critical field which is appreciably smaller than found experimentally and the total number of jumps in the experiment is 19 compared to 11 in the theory. When we enlarge the disk radius from $1.2 \mu\text{m}$ to $1.57 \mu\text{m}$, the number of jumps in the magnetization curve is increased to 19 but the upper critical field is reduced to 63 G. It is also to be noted that the slope of the experimental curve decreases with increasing field and tends to become parallel to the field axis at higher magnetic fields. In finite systems the Bean-Livingston barrier [9] at the surface can cause the system not to evolve along the free energy minimum. It leads to jumps in the magnetization at a much larger value of the magnetic field compared to the value at which the $L = 1$ state becomes the ground state. We have to decrease the width of the disk to an unreasonable value of $0.06 \mu\text{m}$ in order to have the first jump at the same position as that seen in the experiment for the same disk radius. But, as discussed before, such a decrease in thickness does not increase the critical field and cannot explain the high field discrepancy. It is also known that surface defects can destroy the Bean-Livingston barrier for increasing fields.

This work is supported by Flemish Science Foundation (FWO-VI) Grant No. G.0232.96, the European INTAS-93-1495-ext project, and the Belgian Inter-University Attraction Poles (IUAP-VI). One of us (P.S.D.) is supported by the University of Antwerp.

*Electronic address: deo@uia.ua.ac.be

†Permanent address: Institute of Theoretical and Applied Mechanics, Russian Academy of Sciences, Novosibirsk 630090, Russia.

‡Electronic address: peeters@uia.ua.ac.be

- [1] O. Buisson *et al.*, Phys. Lett. A **150**, 36 (1990).
- [2] V.V. Moshchalkov *et al.*, Nature (London) **373**, 319 (1995).
- [3] A.K. Geim *et al.*, Superlattices Microstruct. **21**, (1997); A.K. Geim *et al.*, Nature (London) (to be published); A.K. Geim *et al.*, Appl. Phys. Lett. **71**, 2379 (1997).
- [4] R. Benoist and W. Zwerger, Z. Phys. B **103**, 377 (1997).
- [5] V.V. Moshchalkov, X.G. Qiu, and V. Bruyndoncx, Phys. Rev. B **55**, 11 793 (1997).
- [6] D. Saint-James and P.G. de Gennes, Phys. Lett. **7**, 306 (1963).
- [7] G. Dolan, J. Low Temp. Phys. **15**, 133 (1974).
- [8] B. Spivak and F. Zhou, Phys. Rev. Lett. **74**, 2800 (1995).
- [9] C.P. Bean and J.D. Livingston, Phys. Rev. Lett. **12**, 14 (1964).